Energies **2014**, *7*, 8217-8235; doi:10.3390/en7128217

OPEN ACCESS

energies

ISSN 1996-1073

www.mdpi.com/journal/energies

Article

Advanced Energy Harvesting from Macroalgae—Innovative Integration of Drying, Gasification and Combined Cycle

Muhammad Aziz *, Takuya Oda and Takao Kashiwagi

Solutions Research Laboratory, Tokyo Institute of Technology, 2-12-1 Ookayama, Meguro-ku, Tokyo 152-8550, Japan; E-Mails: oda@ssr.titech.ac.jp (T.O.); kashiwagi@ssr.titech.ac.jp (T.K.)

***** Author to whom correspondence should be addressed; E-Mail: maziz@ssr.titech.ac.jp; Tel.: +81-3-5734-3809; Fax: +81-3-5734-3559.

External Editor: Paul L. Chen

Received: 2 October 2014; in revised form: 25 November 2014 / Accepted: 2 December 2014 / Published: 10 December 2014

Abstract: State-of-the-art integrated macroalgae utilization processes, consisting of drying, gasification, and combined cycle, are proposed and their performance with respect to energy efficiency are evaluated. To achieve high exergy efficiency, the integration is performed through two main principles: exergy recovery and process integration. Initially, the energy involved in one process is recirculated intensively through exergy elevation and effective heat coupling. Furthermore, the unrecoverable energy from one process will be utilized in the other processes through process integration. As the result, the total exergy destruction from the whole integrated processes can be minimized significantly leading to significant improvement in energy efficiency. The first analysis relates to the performance of integrated drying process, especially the influence of target moisture content to energy consumption. Furthermore, the influences of gasification fluidization velocity to the total generated power and power generation efficiency are also calculated. As the results of study, the proposed integrated-processes proved a very high energy efficiency. A positive energy harvesting with the total power generation efficiency of about 40% could be achieved.

Keywords: macroalgae; energy harvesting; drying; gasification; combined cycle; exergy recovery; process integration; energy efficiency

---

1. Introduction

Algae are believed as one of promising candidates for a broad range of application including goods production and green energy resource. They have attracted a lot of interest for energy production due to their high potential and positive characteristics. Wang *et al.* [1] stated that algae have a high capability of photosynthetic fixation of CO_2 for generation of various algal cell components, energy and molecular oxygen. In addition, algae have some superior features compared to lignocellulosic biomasses due to their higher growth rates, no need for abundant fresh water for irrigation, the capability to grow under conditions that are not favorable for terrestrial biomasses, potential for sustainable growth by extracting macro- and micro-nutrients from wastewater and industrial flue stack emissions, *etc*. Algae have a more efficient solar energy conversion and nutrient acquisition, hence they have a higher rate of productivity per unit of area compared to traditional terrestrial crops such as corn and soybean [2,3]. Algae can be grown anywhere, even in sewage, salt water, *etc*., do not require fertile land and produce larger energy than which is required for the conversion processes [4].

The cultivation of algae is however usually limited by some factors, including the availability of water, nutrients, CO_2, sunlight, temperature, *etc*. Co-location of algae cultivation facilities near CO_2 emitting industrial points is potentially a very positive strategy to grow large quantities of algal biomass and also to recycle the exhausted CO_2 for fuel production. As the algae grow in aqueous environments, the most efficient way of capturing CO_2 is by directly passing the flue gas though the culture medium [5]. The flue gas exhausted from the plants usually contains of CO_2, NO_x, SO_x, Ni, V and Hg. From the previous studies, the emitted NO_x dissolved in the medium has no negative effects on the algal growth because it will be converted into NO_2 and utilized as nitrogen source. In addition, SO_x also shows no harmful effects to the algae as long as its concentration in the flue gas is lower than 400 ppm [6–8]. On the other hand, Ni and V which are typically above 1.0 ppm and 0.1 ppm, respectively, could decrease the algal productivity. Furthermore, Matsumoto *et al.* [9] concluded that algae could be cultivated effectively under high concentrations of CO_2 (approximately 15%).

To harvest the energy from algae, two main conversion technologies can be utilized: thermochemical and biochemical routes. Compared to biochemical conversion, thermochemical conversion generally has advantages of faster conversion rates and more complete conversion to products. In addition, in thermochemical conversion, gasification is considered to have higher conversion efficiency compared to other processes, including pyrolysis, *etc*. [3]. Furthermore, gasification of algae can be performed through conventional gasification and supercritical water gasification. In contrast to supercritical water gasification, which is still at the research and development stage, conventional gasification of biomass to produce syngas has been well developed in recent decades. Unfortunately, for conventional gasification, the harvested algae must be dried to a low moisture content to maintain the conversion process stable and efficient. For example, to achieve a gasification temperature of 900 ℃, generally biomass needs to be dried to a moisture content of about 10 wt% on a wet basis (wb).

Power generation is considered a promising method to harvest the energy from biomass. Biomass-based power generation, as well as hydro and geothermal energy, is expected to be able to replace the current base load power plants which are mainly supplied by fossil fuels and nuclear. Power generation from algae can be performed through co-combustion with other fuels such coal, *etc.*, or independently by direct combustion or combinations of conversion technologies and power generation, such as

integrated gasification and combined cycle (IGCC). IGCC is considered the most efficient way to generate electricity due to its high carbon conversion, high power generation efficiency and low environmental impact [10].

Although the potential of algae as an energy source is very high, to the best knowledge of the authors, almost no study has focused on the topic of how to effectively generate electricity from algae. In addition, algae have a very high moisture content ranging from 70 wt% wb to 90 wt% wb leading to some barriers in their utilization. Drying is one method to improve their concentration leading to higher calorific value. This study proposes the integrated energy utilization of algae, especially macroalgae, for power generation with high total energy efficiency. To achieve it, an integrated drying, gasification and combined cycle process is proposed based on a combination of exergy recovery and process integration technologies.

2. Integrated Drying, Gasification, and Combined Cycle

In this study, to achieve high energy efficiency in integrated drying, gasification, and combined cycle, a technological combination of exergy recovery and process integration is initially proposed. In conventional process integration, heat integration among processes is conducted basically through a pinch technology or heat cascade utilization. Hence, the energy involved in the process cannot be recovered effectively, thus still causing large amount of exergy destruction in the whole processes. In the proposed combined exergy recovery and process integration, the heat involved in the whole processes is thoroughly recovered. Exergy recovery is employed in each process to circulate the heat involved in the same process. Theoretically, to achieve it, exergy elevation and effective heat coupling are conducted. First, the exergy of the process stream is elevated by means of compression before performing a heat exchange between the hot and cold streams. Second, to achieve a maximum balanced heat, heat coupling for each type of heat is performed. This includes some different types of heat: sensible, latent, endothermic, and exothermic heats. Aziz *et al.* have studied the application of exergy recovery technology in standalone drying process for algae [11], low rank coal [12], and empty fruit bunches [13]. They showed that significant improvement in total energy efficiency could be achieved, hence, the total energy required for drying was reduced significantly.

Unfortunately, in the process with high energy (heat) circulation, there are still some energy losses due to the heat exchanger limitations, *etc.* To utilize the unrecoverable energy (heat) in one process, the idea of process integration is introduced. In process integration, the unrecoverable energy (heat) from one process will be utilized in other processes. Hence, the total energy loss in the integrated processes could be further reduced.

The proposed integrated-processes consists of drying, gasification and combined cycles. Figure 1 shows the energy and material circulations in the integrated energy harvesting processes for macroalgae. The materials are basically circulated resulting in power generation with minimum CO_2 emissions. Starting from cultivation, macroalgae are cultivated in some water-based environment such as an ocean, artificial pond, artificial reactor, *etc.* The harvested macroalgae from the cultivation having high moisture content flow to a drying module to reduce their moisture content, hence, their calorific value is improved. Subsequently, the hot dried-macroalgae are used in the gasification module and are thus converted to syngas consisting of hydrogen, methane, carbon monoxide, *etc.* Among the available biomass conversion technologies, gasification can rapidly convert the whole macroalgae including cellulose,

hemicellulose and lignin. After gas treatment, the produced syngas flows to the combined-cycle-based power generation comprising combustor, gas turbine, heat recuperator and steam turbine. A part of the generated electricity is consumed internally for cultivation, drying and gasification. Moreover, a CO_2-rich flue gas exhausted from the power generation module is recycled and utilized for both heat and materials in drying and cultivation, respectively. Basically, the heat of flue gas is utilized for preheating the wet macroalgae. Moreover, the chemical components of flue gas can be utilized as nutrients for macroalgae to grow. Figure 2 shows the detailed schematic diagram of the proposed integrated-processes including drying, gasification, and combined cycle.

Figure 1. Energy and material circulations in the proposed integrated-processes.

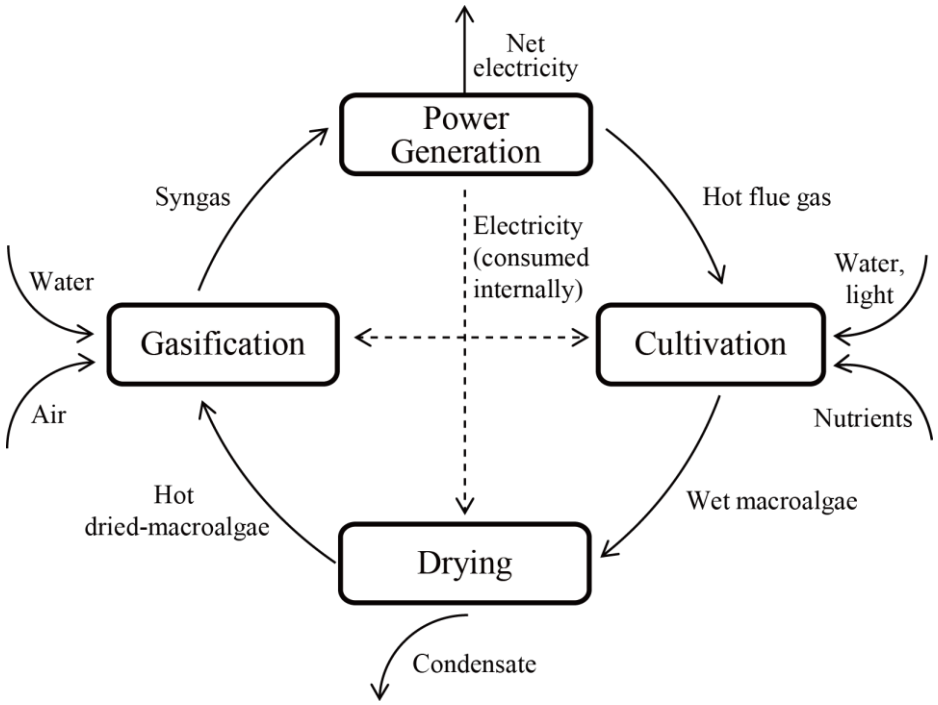

Figure 2. Process flow diagram of the proposed integrated-processes for macroalgae consisting of drying, gasification, and combined cycle.

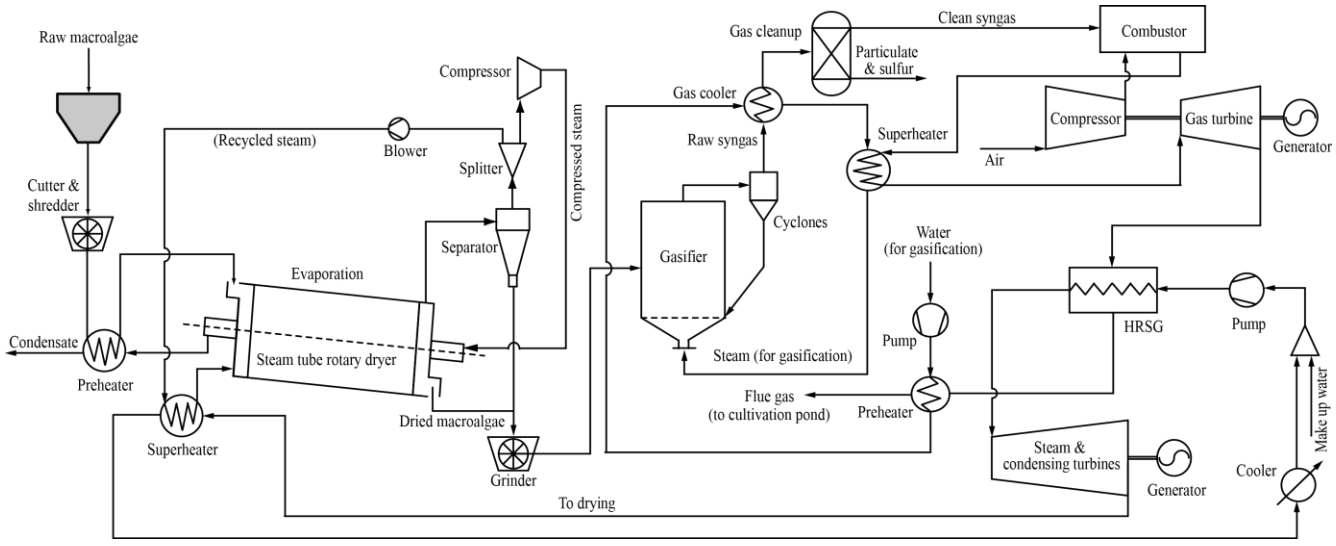

2.1. Macroalgae Drying

In the proposed integrated-drying process, a preheater, a main dryer (steam tube rotary dryer), and a superheater are required. Before entering the preheating stage, the wet macroalgae enter the pre-treatment stage (cutting, *etc.*) to achieve a uniform size, decrease their long filamentosity and improve their dynamics in the dryer, hence, a better and more uniform heat transfer, as well as uniform moisture removal rate, can be achieved. In the preheating stage, wet macroalgae are preheated to a certain temperature near its saturation point utilizing the sensible heat of the condensed water of the compressed steam flowing out from steam tube rotary dryer. In this stage, a sensible heat exchange is conducted between wet macroalgae as cold stream and condensed water from compressed steam as a hot stream. Furthermore, the cold condensed water exhausted from the preheater is treated before it can be used as the steam source required in gasification stage.

Next, the wet macroalgae enter the evaporation stage which is performed in the steam tube rotary dryer. In this study, to facilitate an effective heat exchange inside the dryer, a steam tube rotary dryer with an internal heat exchangers is considered to be the most appropriate candidate for macroalgae drying. Some advantages of the steam tube rotary dryer include a large heat transfer area leading to high thermal efficiency, excellent drying control, comfortable handling capability, easy implementation for continuous operation, *etc.* [11]. The heat exchange inside the rotary dryer could also be set up in counter current mode, whereby macroalgae and compressed steam are flowing in opposite directions to each other and hence, the minimum temperature difference inside the dryer could be minimized. This is different from concurrent heat exchangers such as fluidized beds in which the minimum temperature difference inside the dryer is quite large due to material mixing. Moreover, in a steam tube rotary dryer, heat is mainly exchanged in conductive mode from the heating tubes to the wet macroalgae, although there is the possibility of heat exchange in radiant mode.

The heating tubes inside the rotary dryer are filled with compressed steam having a high exergy rate and arranged in a concentric circle inside the dryer. The heating tubes rotate along with the rotary dryer. These heating tubes supply the heat required for drying, especially the latent heat which is the largest amount of heat required to remove the water from macroalgae. On the other hand, the wet macroalgae are fed continuously at a uniform rate and are tumbled and agitated by the rotation of the rotary dryer. Furthermore, the rotary dryer is designed to have a slope rotating cylinder, hence, it is able to move the macroalgae inside the dryer from the feeding inlet to the discharging outlet by gravitational force, and as a result, the dried macroalgae will be discharged from the outlet.

In this drying stage, the main drying process which is water evaporation is performed utilizing compressed steam as the main heat source. In the steam tube rotary dryer, the heat of condensation of the compressed steam is exchanged with the heat of evaporation of the moisture inside the wet macroalgae. In the dryer, the macroalgae being dried are flowing down through the dryer and finally they are discharged through discharge outlet at the lower end of the dryer. On the other hand, the evaporated water will be exhausted from a different outlet and transported to a filter before it is split at a splitter into recirculated and purged steams. The amount of purged steam is equivalent to the water evaporated from the wet macroalgae. It will be compressed by a compressor to increase its exergy rate. Based on the pressure-enthalpy (p-h) diagram of water, as the pressure increases, the saturation temperature of the water/steam will increase gradually until it reaches the critical point. By compression,

the temperature, as well as the saturation temperature, of the steam exhausted from the dryer will increase, leading to a higher steam exergy rate. The objective of compression is to increase the exergy rate of the steam creating a temperature difference to facilitate a heat exchange between the hot stream (compressed steam) and the cold stream (wet macroalgae). As a result, both the sensible and latent heats of stream can be recovered effectively. The amount of exergy increase will depend strongly on the minimum temperature difference required for the heat exchange. The higher exergy rate of the compressed steam is then recycled and utilized as the heat source for the subsequent drying and preheating stages. Finally it is exhausted as condensate.

On the other hand, the amount of recirculated steam is fixed and constant. It will be recirculated back to the steam tube rotary dryer. For recirculation, a blower is installed. The main purpose of recirculating the steam is to enhance the drying performance including the uniformity of heat exchange and moisture removal and faster drying rate. Hence, the heat exchange in the steam tube rotary dryer is basically conducted in two ways: convective heat transfer (from the recirculated steam) and conductive heat transfer (from the compressed steam inside the heating tubes).

2.2. Gasification and Combined Cycle

To convert macroalgae to syngas, the main gasification reactions to be considered consist of the water-gas reaction, Boudouard reaction, shift reaction, and methanation. A fluidized bed type gasifier is adopted due to its high mass and heat transfer characteristics, high efficiency, high heating value, *etc.* In some literatures, gasification of macroalgae could be achieved through conventional thermal gasification and supercritical water gasification. Unfortunately, supercritical water gasification still faces some engineering problems which need further research and development to be applicable in macroalgae gasification. The problems include continuous feeding, plugging, energy consumption [14,15]. Hence, in this study, thermal gasification is selected to gasify the dried macroalgae. Macroalgae are quickly mixed once they are fed into the gasifier and heated up instantaneously to the gasification temperature. Pyrolysis occurs very quickly, resulting in a high carbon conversion efficiency.

Generally, gasification produces some combustible gases through a series of thermochemical reactions. During the gasification, macroalgae will be converted to a H_2, CO and CH_4-rich syngas. The produced hot syngas flows to cyclones for particle separation before it is cooled down to preheat the steam as fluidizing gas for gasification. Subsequently, the syngas will be cleaned up, removing the particulates and sulfur to achieve a clean syngas. The clean syngas is then used as fuel for combustion in the combustor, creating a high temperature pressurized gas to rotate the gas turbine. As the temperature of the flue gas from the gas turbine is still high (ranging from 600 ℃ to 900 ℃), the rest of the heat will be utilized to evaporate the water in the heat recovery steam generator (HRSG). The steam generated in the HRSG, is subsequently used to rotate the steam turbine to generate the electricity. Furthermore, the condensed water from the steam turbine flows to the drying module for preheating before it is recirculated back to the combined cycle module.

3. Process Calculation

In this study, brown alga *Laminaria digitata* (Oarweed) was selected as the sample due to its high proportion of carbohydrates and low ash content [16]. This type of brown seaweed can grow up to 2 m

in length, having claw-like holdfast, flexible stipes, and a laminate blade up to 1.5 m long split into finger-like segments. The initial moisture content and flow rate of wet *Laminaria digitata* are 80 wt% wb and 100 t h^{-1}, respectively. Table 1 shows the properties of the *Laminaria digitata* sample used, including both proximate and ultimate analyses. In fact, as *Laminaria digitata* is a seasonal kelp, the amounts of volatile matter and ash change according to the harvesting time. Hence, in this study, the average values throughout the year are used.

Table 1. Proximate and ultimate analyses of *Laminaria digitata* used during system calculation.

Properties	Component	Value
Proximate analysis	Volatile matter (wt% db)	64.1
	Ash (wt% db)	21.1
Ultimate analysis	Carbon (wt% db)	33.3
	Hydrogen (wt% db)	5.1
	Nitrogen (wt% db)	1.7
	Sulfur (wt% db)	0.9
	Oxygen (wt% db)	37.8
Calorific value (MJ kg^{-1})		13.8

Table 2 shows the assumed drying conditions used during the process calculations. A steam tube rotary dryer is assumed, consisting of a mixer, a heat exchanger, and a separator. Heat exchange inside the dryer is counter-current. The pressures inside the dryer and the exhausted steam from the dryer are atmospheric. In this study, to evaluate the effect of target moisture content to the energy required for drying, target moisture contents are set to be lower than 40 wt% wb with an interval of 5 wt% wb.

Table 2. Assumed drying conditions for macroalgae used during simulation in the proposed integrated-processes.

Properties	Parameters	Value
Drying	Wet macroalgae flow rate (t h^{-1})	100
	Initial moisture content (wt% wb)	80
	Target moisture content (wt% wb)	5, 10, 15, 20, 25, 30, 35, 40
System	Compressor polytropic efficiency (%)	87
	Heat exchanger minimum temperature difference (℃)	10
	Heat exchanger pressure drop (%)	2

Figure 3 shows the process flow diagram of the proposed drying process for macroalgae developed based on combined exergy recovery and process integration. To facilitate an optimum exergy recovery, a compressor, CP1, and three heat exchangers, HX1, HX2, and HX3, are installed. Wet macroalgae, S1, are initially preheated in the preheater, HX1, by condensed compressed-steam, S8. Next, the preheated macroalgae, S2, enter the steam tube rotary dryer, consisting of a mixer, MX1, heat exchanger, HX2, and separator, SEP1, for water evaporation. The exhausted steam from the steam tube rotary dryer is going to a splitter, SPL1, and is divided into recirculated stem, S10, and purged steam, S6. The purged steam is then compressed by a compressor, CP1, to increase its exergy. Subsequently, the high exergy

rate of the compressed steam, S7, is utilized as the heat source for subsequent drying in HX2 and HX1. On the other hand, the recirculated steam, S10, flows to the blower, BL1, and is superheated by the condensate from the steam turbine, S13, before being recirculated to steam tube rotary dryer. Moreover, the hot dried macroalgae, S15, are fed directly to gasifier.

Figure 3. Process flow diagram of drying module in the proposed integrated-processes.

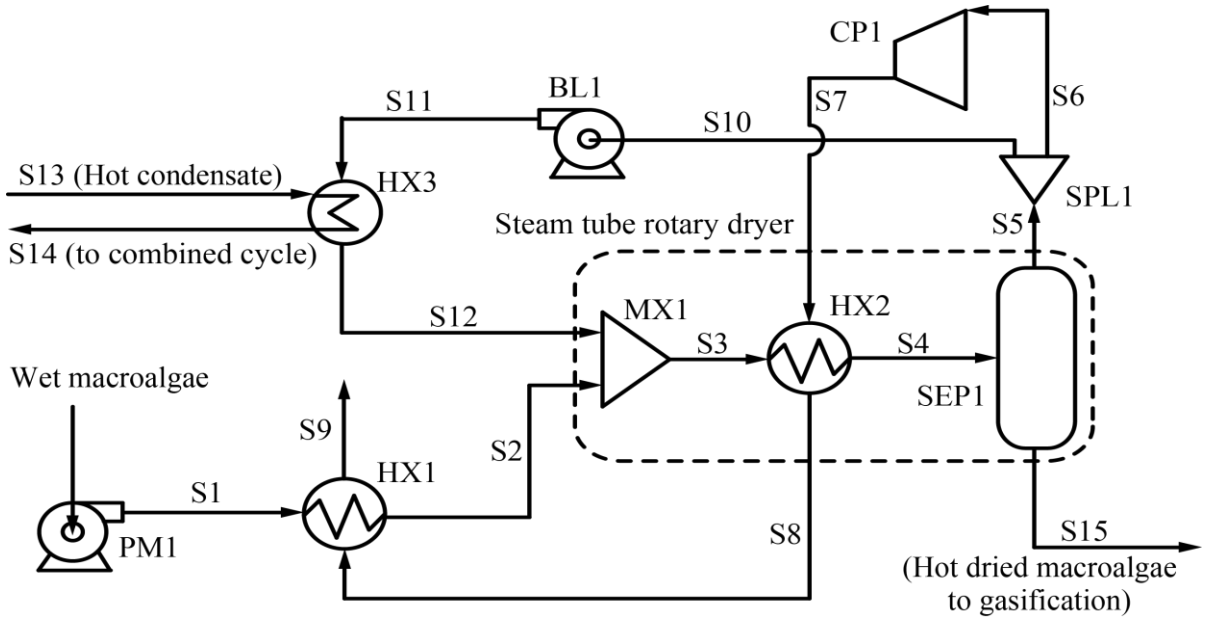

Drying is a complicated moisture removal process because it deals not only with the free water inside the material, but also water held in capillaries and chemically bound water. Therefore, drying to a specific moisture content depends strongly on the equilibrium moisture content, which in turn is dependent on the moisture content of the environment. An equilibrium moisture content changes dynamically depending on the surroundings, especially temperature, humidity, and pressure. In the case of drying with steam, the equilibrium moisture content is strongly influenced by the relative vapor pressure, p/p_{sat}, which is the ratio of the partial vapor pressure to the saturated vapor pressure. A lower relative vapor pressure leads to a stronger driving force for drying, resulting in a lower moisture content of the dried product. In this study, the equilibrium moisture content, MC_{eq}, of *Laminaria digitata* is approximated as follows [17]:

$$MC_{eq} = \frac{1.0078 e^{\left(\frac{-1076}{RT}\right)} e^{\left(\frac{15261}{RT}\right)} \left(\frac{p}{p_{sat}}\right)}{\left[1-1.3638 e^{\left(\frac{-1076}{RT}\right)} \left(\frac{p}{p_{sat}}\right)\right]\left[1-1.3638 e^{\left(\frac{-1076}{RT}\right)} \left(\frac{p}{p_{sat}}\right)+0.1124 e^{\left(\frac{-1076}{RT}\right)} e^{\left(\frac{15261}{RT}\right)} \left(\frac{p}{p_{sat}}\right)\right]} \quad (1)$$

where R and T are gas constant (8.314 J mol^{-1} K^{-1}) and temperature (K), respectively.

The heat transfer inside steam tube rotary dryer is conducted in both convection and conduction modes. The product of the overall heat transfer coefficient, U, and surface area, A, may be approximated by following equation:

$$\frac{1}{UA} = \frac{1}{A_c \alpha_c} + \frac{\ln\left(r_{out}/r_{in}\right)}{2\pi L \lambda_t} + \frac{1}{\alpha_t A_t} \quad (2)$$

where A_c, α_c, L, r_{out}, r_{in}, λ_t, α_t and A_t are condensation surface area (m^2), heat transfer coefficient following condensation (W m^{-2} K^{-1}), tube length (m), tube outer diameter (m), tube inner diameter (m), tube thermal conductivity (W m^{-1} K^{-1}), heat transfer coefficient following heat transfer from tube to drying particles (W m^{-2} K^{-1}), and total tube outer surface area (m^2).

The first term in the right side of Equation (2) represents the heat transfer following two-phase condensation inside the tubes. The second term corresponds to the conductive heat transfer through the heat transfer tubes. In addition, a convective heat transfer from the outer surface of the heat transfer tubes to the particles inside the rotary dryer is expressed by the third term.

The heat transfer coefficient inside steam tube rotary dryer can be approximated by the correlation proposed by Borodulya *et al.* [18–20] as follows:

$$Nu_t = 0.74\, Ar^{0.1}\left(\frac{\rho_p}{\rho_v}\right)^{0.14}\left(\frac{C_p}{C_v}\right)^{0.24}\upsilon_p^{2/3} + 0.46\, Re\, Pr\frac{\upsilon_p^{2/3}}{\upsilon_v} \tag{3}$$

$$Nu_t = \frac{\alpha_t\, d_p}{\lambda_v} \tag{4}$$

where *Nu*, *Ar*, and *Re* are Nusselt, Archimedes and Reynolds numbers, respectively. Furthermore, ρ_p, ρ_v, C_p, C_v, ν_p, ν_v, d_p and λ_v are particle density (kg m^{-3}), steam density (kg m^{-3}), particle heat capacity (kJ kg^{-1} K^{-1}), steam heat capacity (kJ kg^{-1} K^{-1}), particle volumetric fraction (-), steam volumetric fraction (-), particle diameter (m) and steam thermal conductivity (W m^{-1} K^{-1}), respectively.

In addition, the mean heat transfer coefficient following the two-phase complete condensation of the compressed steam can be approximated using a general correlation proposed by Shah [21], based on the Dittus-Boelter equation as follows:

$$\alpha_c = \frac{0.023\, Re_l^{0.8}\, Pr_l^{0.4}\,\lambda_l}{2r}\left[0.55 + 2.09/\Delta p_t^{0.38}\right] \tag{5}$$

where λ_l and Δp_t are liquid thermal conductivity (W m^{-1} K^{-1}) and pressure loss inside the tube (Pa), respectively.

Moreover, the electrical energy consumed in the rotary dryer consists of motor power to drive the rotary dryer and blower work to compensate the pressure loss in the rotary dryer. The motor power, W_{mot}, can be calculated by the following equation [22]:

$$W_{mot} = \frac{N_{rot}\left[34.35\, D_{RD}\, w + 0.424\,(3.28\, D_{RD} + 2)\, w_{rot} + 0.728\, w_{rot}\right]}{735499} \tag{6}$$

where N_{rot}, D_{RD}, w, and w_{rot} are rotational speed (rpm), dryer diameter (m), live load (kg), and total rotating load (kg), respectively.

On the other hand, the pressure drop across the rotary dryer, Δp_{RD}, resulting in the blower work, W_{BL}, can be calculated as follows [22]:

$$\Delta p_{RD} = \left[\frac{4 f\left(n_t + 1\right)^{D_s G_s^2}}{2 D_e \rho_v}\right] \times 0.5 \tag{7}$$

$$f = 1.87\left(\frac{G_s D_e}{\mu_v}\right)^{-0.2} \quad (8)$$

where D_s, D_e, μ_v and G_s are baffle spacing (m), equivalent diameter (m), steam dynamic viscosity (Pa s), and mass flux (kg m^{-2} s^{-1}), respectively.

The total energy input for drying, $W_{dry,tot}$, can be defined as the sum of all works involved in in the proposed integrated-drying process which can be written as follows:

$$W_{dry,\,tot} = W_{CP1} + W_{BL1} + W_{PM1} + W_{mot} \quad (9)$$

where W_{CP1}, W_{BL1} and W_{PM1} are compressor, blower and pump works used in drying module, respectively.

Table 3 shows the gasification conditions assumed in this study. To improve the conversion efficiency during gasification, Fe_2O_3-90% CeO_2 is simultaneously used as catalyst and fluidizing medium. The gasification conditions and composition of the produced syngas are basically based on the work of Duman *et al.* [23]. The utilization of Fe_2O_3-CeO_2 as catalyst can convert the produced tar completely, hence, a significant improvement of gasification efficiency can be achieved. This catalyst can enhance the water gas shift reaction during gasification. Iron-based catalysts are known to be good oxygen carriers and they have relatively good stability during the reaction [24,25]. Furthermore, the fluidizing medium is expected to increase the fluidization performance of the macroalgae particles due to more uniform temperature distribution across the bed.

Table 3. Assumed gasification conditions used during calculation including syngas composition and fluidizing particles inside the gasifier.

Properties	Component	Value
Temperature (℃)		700
Syngas composition	H_2 (m^3 kg-dried macroalgae^{-1})	0.937
	CO (m^3 kg-dried macroalgae^{-1})	0.052
	CH_4 (m^3 kg-dried macroalgae^{-1})	0.081
	CO_2 (m^3 kg-dried macroalgae^{-1})	0.538
Fluidizing particle	Material	Fe_2O_3-90% CeO_2
	Average particle size (mm)	0.367
	Density (kg m^{-3})	1000
	Surface area (m^2 g^{-1})	22
	Sphericity (-)	0.85
	Voidage at minimum fluidization (-)	0.45

Figure 4 shows the process flow diagram of gasification and combined modules in the proposed integrated-processes. Hot dried macroalgae enter the gasifier, GF, to be converted to syngas, S16. The heat of the hot syngas is utilized to generate steam for gasification/fluidization in HX4. Next, cold syngas is cleaned before it is used as fuel for combustion in the combustor, CB. The hot gas from the combustor is then utilized initially to superheat the steam for gasification in HX5 before it expands in the gas turbine, GT, to rotate the generator. The heat of the hot flue gas from the gas turbine is recovered to generate steam in HRSG to rotate the steam turbine, ST, producing additional power generation. The condensate exhausted from the steam turbine, S13, flows to the drying module which is used to superheat the

recirculated steam. The steam for gasification/fluidization is supplied by feeding water, S26, which is initially preheated in HX6 using the heat of the flue gas exhausted from HRSG, S22.

Figure 4. Process flow diagram of gasification and combined cycle modules in the proposed integrated-processes.

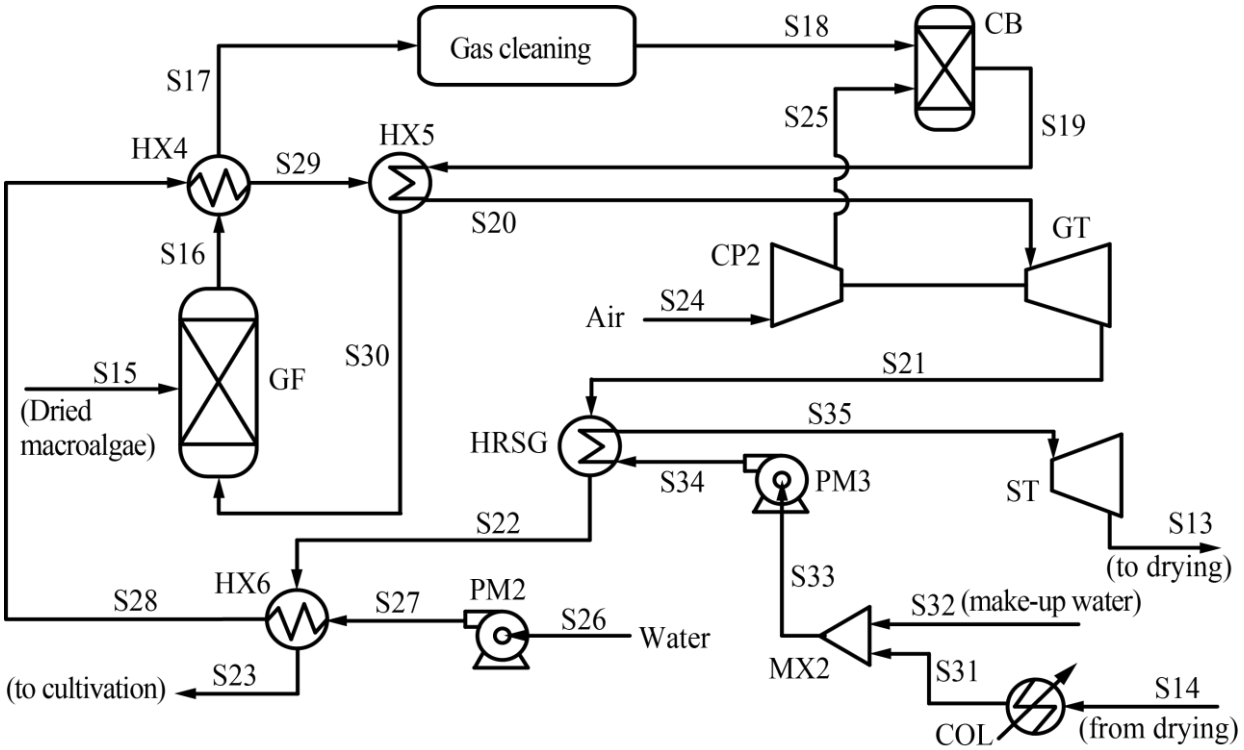

As Fe_2O_3-90% CeO_2 acts as catalyst and fluidizing medium, the minimum fluidization velocity of the bed, U_{mf}, is approximated as the minimum fluidization of fluidizing medium. This is approximated by the modified Ergun equation for small particles as follows [26]:

$$U_{mf} = \frac{d_m{}^2 (\rho_m - \rho_v) g}{150 \mu_v} \left(\frac{\varepsilon_{mf}^3 \Phi_m^2}{1 - \varepsilon_{mf}} \right) \quad (10)$$

where d_m, ρ_m, g, ε_{mf}, and Φ_m are fluidizing particle diameter (m), density (kg m^{-3}), acceleration due to gravity (m s^{-2}), void fraction (-) and sphericity (-), respectively.

Furthermore, the pressure drop required for fluidization, Δp_{fl}, is calculated as the sum of pressure drop across the bed and pressure drop due to distribution plate. Moreover, the pressure drop due to distribution plate is assumed to be 0.4 of pressure drop across the bed. Hence, total pressure drop required for fluidization, Δp_{fl}, can be shown as follows:

$$\Delta p_{fl} = 1.4 \left[(1 - \varepsilon_{mf})(\rho_m - \rho_s) H \, g/c \right] \quad (11)$$

where H and c are fluidization height (m) and conversion factor (1 kg m N^{-1} s^{-2}), respectively.

Table 4 shows the assumed conditions used for calculating the combined cycle module used in this study. Furthermore, process modeling and calculation of the proposed drying system, modeling and calculations are conducted using a steady state process simulator, Pro/II version 9.2 (Invensys Corp., London, UK). The fluidized bed gasifier is assumed to consist of a mixer, a heat exchanger, a conversion

reactor, and a separator. Air is considered to consist of 79% nitrogen and 21% oxygen. To evaluate the total energy efficiency of the proposed integrated-processes, the impact of steam fluidization velocity to the total generated power and power generation efficiency are calculated. Three different fluidization velocities are evaluated: 3, 4 and 5 U_{mf}.

Table 4. Assumed conditions used during simulation for combined cycle including the gas and steam turbines. HRSG: heat recovery steam generator.

Properties	Parameters	Value
Combustor and gas turbine	Compressor outlet pressure (MPa)	2
	Compressor polytropic efficiency (%)	87
	Combustor pressure drop (%)	2
	Gas turbine inlet temperature (℃)	1300
	Gas turbine adiabatic efficiency (%)	90
	Air to fuel ratio (-)	10
HRSG and steam turbine	HRSG outlet pressure (MPa)	10
	Heat exchanger temperature difference (℃)	10
	HRSG pressure drop (%)	1
	Steam turbine polytropic efficiency (%)	90
	Minimum outlet vapor quality (%)	90

4. Results and Discussion

4.1. Drying Performance of the Proposed Integrated-Drying Process

Figure 5 shows the correlation of total required energy and compressor outlet pressure corresponding to the target moisture content of the drying step, respectively. In drying to a target moisture content of higher than 20 wt% wb, the higher target moisture content leads to significantly higher total required energy in the proposed integrated-drying system. This phenomenon is caused mainly by the material imbalance. As the target moisture content increases, the amount of compressed steam decreases accordingly. Principally, in a steam tube rotary dryer, the energy (heat) for drying including sensible and latent heats of water and sensible heat of solid are covered by the heat of the compressed steam. Hence, as the amount of macroalgae is constant, a smaller amount of compressedsteam will require a higher compression ratio to provide the required heat for drying. On the other hand, when drying has progressed to below 20 wt% wb, the total required energy for drying becomes higher although in an insignificant way. This phenomenon is considered to be due to ineffective heat exchange between the hot stream (compressed steam) and cold stream (macroalgae) resulting in larger exergy destruction. In drying with a target moisture content of less than 20 wt% wb, the relative vapor pressure, which is the driving force for drying, must be reduced following the decrease of target moisture content. As the pressure during drying is constant for all target moisture contents, the lower relative vapor pressure leads to a significant increase of the drying temperature. Compared to drying to a moisture content of 10 wt% wb, drying to moisture content of 5 wt% wb requires an about 31 ℃ higher drying temperature. This significant temperature increase causes an increase in the compressor and blower duties, hence the total required energy increases.

Figure 5. Correlation between the total required energy and compressor outlet pressure with the target moisture content.

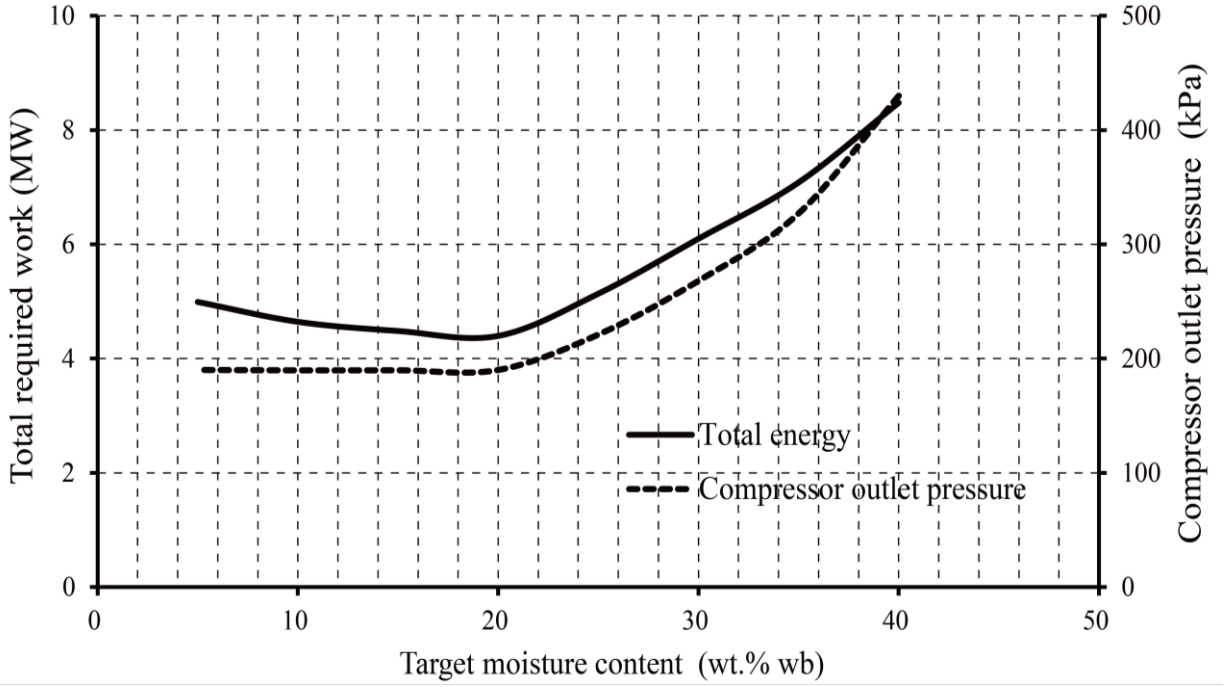

Compared to compressor work, both the pump and motor work are significantly smaller and their values are almost constant under all evaluated drying conditions. Moreover, regarding the blower work, since the flow rate of the recirculated steam is fixed and the same in all drying condition cases, the blower work depends on the temperature of the recirculated steam, which is the same as the drying temperature. The blower work increases following the decrease of target moisture content due to higher steam temperature, but as the pressure increase produced by blower is relatively lower compared to the compressor, there is no significant change in the blower work under all evaluated target moisture contents. Hence, the change of total required energy is mainly due to the change of the steam compression work by the compressor.

Based on Figure 5, drying to a moisture content of 10–20 wt% wb is considered as the most feasible way to upgrade the calorific value of macroalgae in terms of energy efficiency. For gasification, generally, a higher gasification temperature leads to higher conversion efficiency. Furthermore, to achieve a higher gasification temperature, a lower moisture content of the feedstock is required. According to the report published by the National Renewable Energy Laboratory (NREL) [27], in the case of biomass feedstocks, to achieve a relatively high gasification temperature, the biomass feedstock need to be dried to a moisture content of about 10 wt% wb. Hence, it is believed that drying of macroalgae to a moisture content of 10 wt% wb is the most appropriate drying condition in terms of both energy efficiency of drying and gasification efficiency.

Figure 6 shows the temperature-enthalpy diagram of the proposed drying process in the case of a target moisture content of 10 wt% wb. Solid and dashed lines represent the hot and cold streams, respectively. In the first preheater, HX1, the sensible heat exchange mainly takes place between the compressed steam condensate and the wet macroalgae. Furthermore, the preheated macroalgae enter the dryer, HX2, and are mixed with the recirculated steam, hence, their temperature increases significantly. In HX2, the exchange of latent heat with the compressed steam condensate and evaporation of water from the

wet macroalgae mainly take place. The amount of heat exchange in HX2 is the largest because of the latent heat exchange. In addition, the hot condensate from the steam turbine is coupled with the recirculated water in HX3 for the purpose of superheating, hence, any condensation due to the mixing of hot steam and cold macroalgae inside the dryer can be avoided. Generally, the curves of both hot and cold streams are almost parallel to each other, meaning that the latent heat following the condensation of compressed steam can be recovered effectively and utilized to evaporate the water inside the macroalgae. This effective heat coupling is key to the success of the proposed combined exergy recovery and process integration.

Figure 6. Temperature-enthalpy diagram of the proposed integrated-drying system (in case of target moisture content 10 wt% wb.

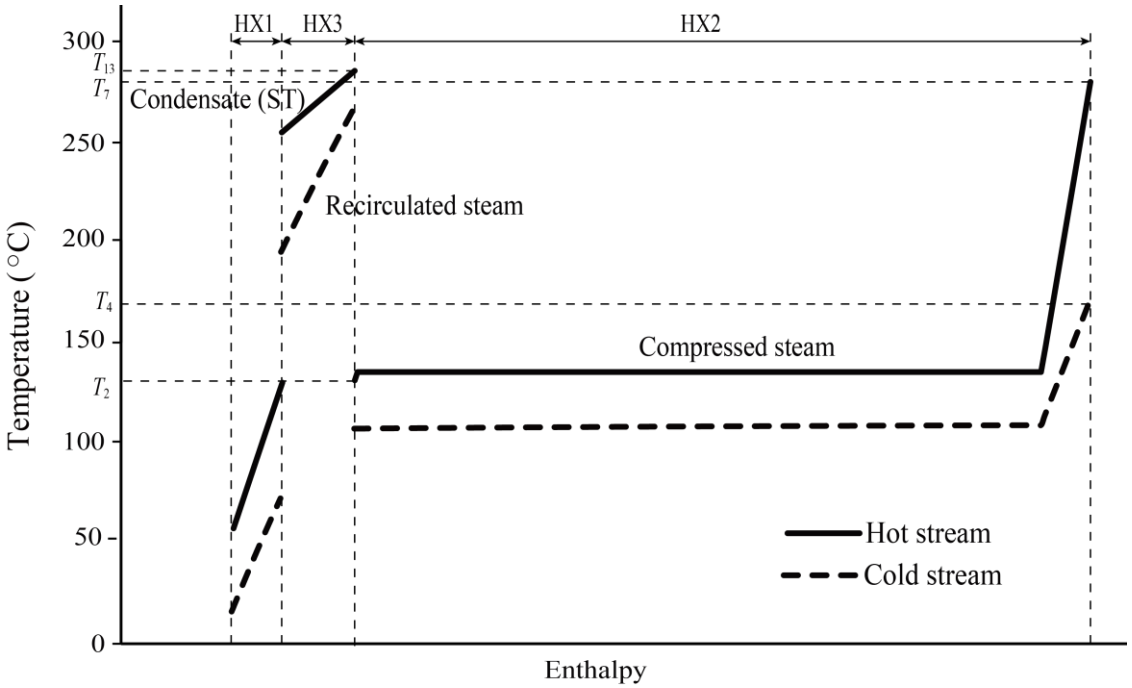

In drying, the exergy loss is generally divided into two types: exergy loss due to separation following drying and exergy loss due to irreversible heat exchange. In this study, as the exergy loss due to separation is inevitable, the exergy analysis is focused on the exergy loss following the heat transfer Ex_{HX} which can be approximated by the following equation [28]:

$$Ex_{HX} = \left(m_v \, \Delta S_v + m_l \, \Delta S_l + m_v \frac{\Delta H_{trs}}{T_{trs}} \right) \Delta T_{min} \quad (12)$$

The first and second terms represent the exergy loss following the sensible heat exchange for each steam and liquid stream, respectively. In addition, the third term represents the exergy loss due to latent heat exchange following the evaporation. ΔH_{trs}, T_{trs} and ΔT_{min} are enthalpy differences following phase transition, phase transition temperature and temperature difference of the heat exchanger, respectively. It is obvious that the exergy loss due to heat transfer depends strongly on the overall average temperature difference throughout the whole process.

The exergy loss due to heat transfer can be reflected by the area between the hot and cold stream lines. As the curves of the hot and cold streams in the overall drying process are almost parallel, the average

minimum temperature difference becomes small. Hence, considering the correlation between the minimum temperature difference and the exergy loss described in Equation (12), the total exergy loss can be minimized. It is obvious that a significant minimization of exergy loss could be achieved by applying the proposed drying technology.

Because the dried macroalgae still have a relatively high temperature, they can be fed to the gasification module directly without having to be cooled down. In addition, the condensed compressed-steam is also relatively hot and can be used as a steam source for the gasification process which will be heated up further by the hot syngas and hot gas from combustors. Hence, the exergy destruction in the overall integrated process (drying, gasification and combined cycle) can be minimized.

4.2. Total Power Generation of the Integrated Processes

Figure 7 shows the relation of fluidization velocity during gasification to the net generated power and total power generation efficiency. In addition, Table 5 shows the detailed both consumed energy and produced energy in the proposed integrated-processes. Consumed energy is the total energy which is consumed in the overall integrated processes, especially by the compressor, blower, and pump. On the other hand, the total produced energy is the total power generated by both the gas and steam turbines. Total power generation efficiency is defined as ratio of net generated power to lower heating value of the fuel feed (raw wet macroalgae). Three fluidization velocities are evaluated: 3, 4, and 5 U_{mf}. This is due to the use of a bubbling fluidized bed to achieve more uniform and faster heat transfer across the bed. As the result of this study, it can be seen that the total generated power and power generation efficiency increased as the fluidization velocity decreased. Furthermore, the total power generation efficiency could reach about 40%, leading to highly positive energy harvesting from macroalgae.

Figure 7. Correlation of fluidization velocity to total generated power and power generation efficiency.

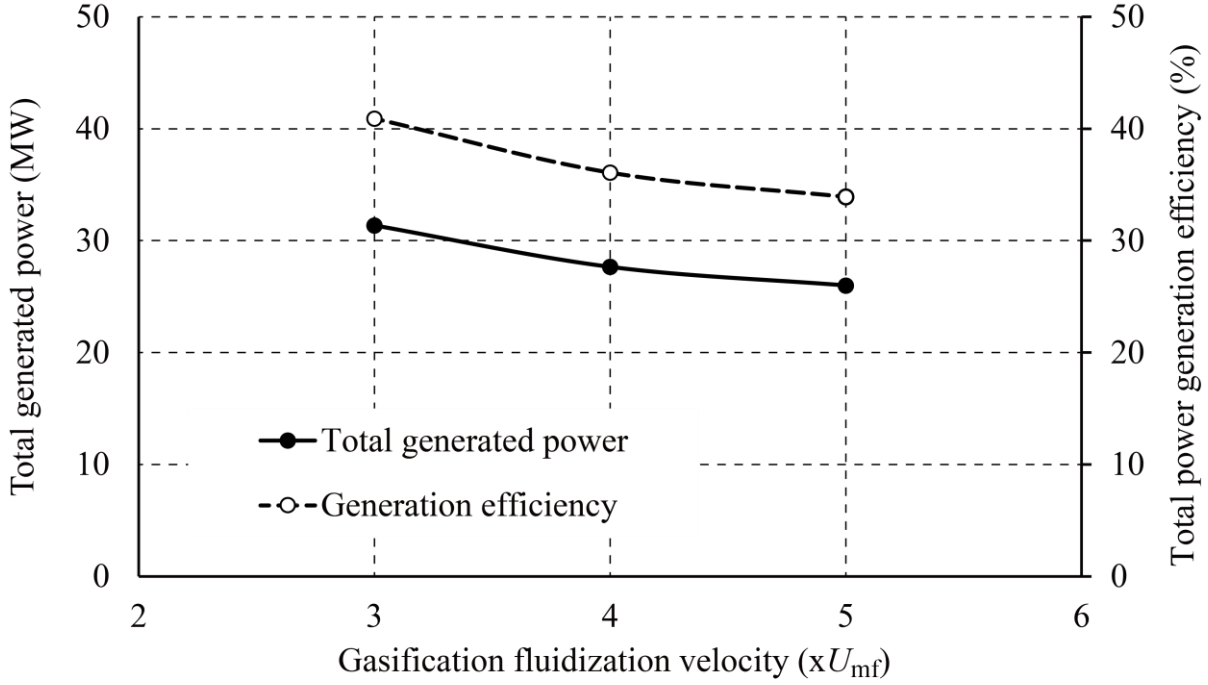

Table 5. Detailed consumed energy and produced energy in the proposed integrated-processes.

Fluidization velocity (x U_{mf})	Algae flow rate (t h^{-1})	Consumed energy (MW)	Produced energy (MW)	Net generated power (MW)	Total power generation efficiency (%)
1	100	19.0	50.4	31.4	41
2	100	28.3	55.6	27.3	36
3	100	34.7	60.7	26.0	34

An exergy increase basically happens twice in the integrated processes. The first exergy increase occurs in drying process where the purged steam is compressed by a compressor creating a high exergy rate in the hot stream utilized as the heat source for the subsequent drying. In this case, a combination of electrical energy and thermal energy is performed, hence the exergy rate of thermal energy can be elevated. The second exergy increase occurs in the gasification module where the steam for gasification/fluidization is superheated by the hot gas from the combustor. In this case, the combination of both thermal energies is performed, hence the exergy rate of thermal energy with lower exergy rate can be elevated.

Based on some literatures [29,30], the productivity of cultivated *Laminaria* sp. is higher than 15,000 g m^{-2} on a dry basis. It should be noted that *Laminaria* sp. is a seasonal macroalga and commonly can be harvested after 7 months of cultivation. Assuming that the algae flow rate is 100 t h^{-1} (as used in this study), and the initial moisture content is 80 wt% wb, for a plant operating 24 h day^{-1}, and 365 days yr^{-1}, the required cultivation area is about 15 km^2.

Figure 8 shows the temperature-enthalpy diagram of the gasification and combined cycle modules in the case where the fluidization velocity is 4 U_{mf}. The hot and cold stream curves are almost parallel to each other, leading to effective heat coupling. Hence, the exergy destruction in the overall integrated processes can be minimized resulting in a high energy efficiency for the integrated system. The largest heat recovery can be achieved in HRSG, followed by heat recovery of hot syngas exhausted from the gasifier (HX4).

Figure 8. Temperature-enthalpy diagram for gasification and combined cycle modules in the integrated processes (fluidization velocity of 4 U_{mf}).

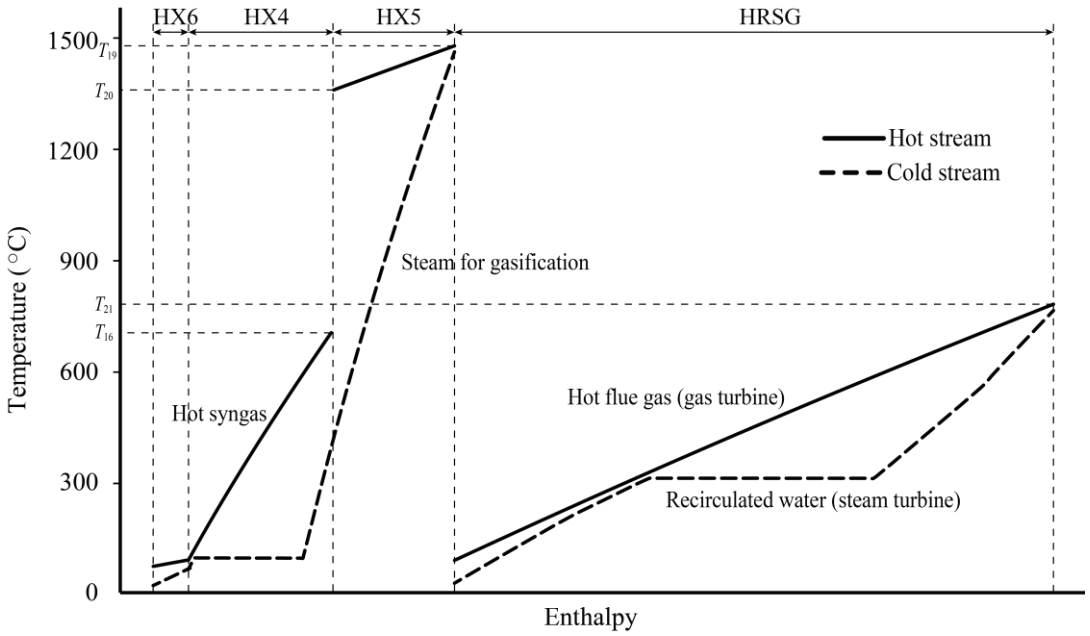

5. Conclusions

A state-of-the-art integrated process for macroalgae including drying, gasification and combined cycle has been proposed based on combined exergy recovery and process integration technologies. Hence, exergy destruction in the whole integrated processes could be minimized and high energy efficiency could be realized. In macroalgae drying, by employing the combined exergy recovery and process integration, the energy required for drying could be reduced significantly. The lowest energy input required for drying could be achieved in the case of a target moisture content of 10–20 wt% wb. Furthermore, the proposed integrated-processes showed relatively high total power generation efficiency, about 40%. It is believed that the integrated processes can increase the overall energy conversion efficiency of algae to power, hence, improve the utilization of algae as high potential energy resource.

Acknowledgments

A part of this research is supported by research development program at Solutions Research Laboratory, Tokyo Institute of Technology, Japan.

Author Contributions

Muhammad Aziz contributed to the overall analysis and preparation of the manuscript. Takuya Oda and Takao Kashiwagi read, revised and approved the manuscript.

Conflicts of Interest

The authors declare no conflict of interest.

References

1. Wang, B.; Li, Y.; Wu, N.; Lan, C.Q. CO_2 bio-mitigation using microalgae. *Appl. Microbiol. Biothechnol.* **2008**, *79*, 707–718.
2. Aziz, M.; Oda, T.; Kashiwagi, T. Integration of energy-efficient drying in microalgae utilization based on enhanced process integration. *Energy* **2014**, *70*, 307–316.
3. Chelf, P.; Brown, L.M.; Wyman, C.E. Aquatic biomass resources and carbon dioxide trapping. *Biomass Bioenergy* **1994**, *4*, 175–183.
4. Demirbas, M.F. Biofuels from algae for sustainable development. *Appl. Energy* **2011**, *88*, 3473–3480.
5. Benemann, J. CO_2 mitigation with microalgal systems. *Energy Convers. Manag*. **1997**, *38*, S475–S479.
6. Matsumoto, H.; Shioji, N.; Hamasaki, A.; Ikuta, Y.; Fukuda, Y.; Sato, M.; Endo, N.; Tsukamoto, T. Carbon dioxide fixation by microalgae photosynthesis using actual flue gas discharged from a boiler. *Appl. Biochem. Biotechnol.* **1995**, *51–52*, 681–692.
7. Vunjak-Novakovic, G.; Kim, Y.; Wu, X.; Berzin, I.; Merchuk, J.C. Air-lift bioreactors for algal growth on flue gas: Mathematical modeling and pilot-plant studies. *Ind. Eng. Chem. Res*. **2005**, *44*, 6154–6163.

8. Yanagi, M.; Yoshitomo, W.; Saiki, H. CO_2 fixation by *Chlorella* sp. HA-1 and its utilization. *Energy Convers. Manag.* **1995**, *36*, 713–716.
9. Matsumoto, H.; Hamasaki, A.; Sioji, N.; Ikuta, Y. Influence of CO_2, SO_2 and NO in flue gas on microalgae productivity. *J. Chem. Eng. Jpn.* **1995**, *30*, 620–624.
10. Aziz, M.; Prawisudha, P.; Prabowo, B.; Budiman, B.A. Integration energy-efficient empty fruit bunch drying with gasification/combined cycle. *Appl. Energy* **2015**, *139*, 188–195.
11. Aziz, M.; Oda, T.; Kashiwagi, T. Enhanced high energy efficient steam drying of algae. *Appl. Energy* **2012**, *109*, 163–170.
12. Aziz, M.; Oda, T.; Kashiwagi, T. Energy-efficient low rank coal drying based on enhanced vapor recompression technology. *Dry. Technol.* **2014**, *32*, 1621–1631.
13. Aziz, M.; Oda, T.; Kashiwagi, T. Innovative steam drying of empty fruit bunch with high energy efficiency. *Dry. Technol.* **2014**, doi:10.1080/07373937.2014.970257.
14. Matsumura, Y.; Minowa, T.; Potic, B.; Kersten, S.R.A.; Prins, W.; van Swaaij, W.P.M.; van de Beld, B.; Elliott, D.C.; Neuenschwander, G.G.; Kruse, A.; *et al.* Biomass gasification in near- and super-critical water: Status and prospects. *Biomass Bioenergy* **2005**, *29*, 269–292.
15. Antal, M.J.; Allen, S.G.; Schulman, D.; Xu, X.D.; Divilio, R.J. Biomass gasification in supercritical water. *Ind. Eng. Chem. Res.* **2000**, *39*, 4040–4053.
16. Adams, J.M.M.; Ross, A.B.; Anastasakis, K.; Hodgson, E.M.; Gallagher, J.A.; Jones, J.M.; Donnison, I.S. Seasonal variation in the chemical composition of the bioenergy feedstock *Laminaria digitata* for thermochemical conversion. *Bioresour. Technol.* **2011**, *102*, 226–234.
17. Mohamed, L.A.; Kouhila, M.; Lahsasni, S.; Jamali, A.; Idlimam, A.; Rhazi, M.; Aghfir, M.; Mahrouz, M. Equilibrium moisture content and heat of sorption of *Gelidium sesquipedale*. *J. Stored Prod. Res.* **2005**, *41*, 199–209.
18. Borodulya, V.A.; Teplitsky, Y.S.; Sorokin, A.P.; Mastnev, V.V.; Markevich, I.I.; Kovenskiy, V.I. External heat transfer in polydispersed fluidzed beds at increased temperature. *J. Eng. Phys.* **1989**, *56*, 767–773.
19. Borodulya, V.A.; Teplitsky, Y.S.; Sorokin, A.P.; Markevich, I.I.; Hassan, A.F.; Yeryomenko, T.P. Heat transfer between a surface and a fluidized bed: Consideration of pressure and temperature effects. *Int. J. Heat Mass Transf.* **1991**, *34*, 47–53.
20. Chen, J.C. Heat transfer in fluidized beds. In *Fluidization, Solids Handling, and Processing*; Yang, W.C., Ed.; William Andrew Publishing: New York, NY, USA, 1998; pp. 153–208.
21. Shah, M.M. A General correlation for heat transfer during film condensation in pipes. *Int. J. Heat Mass Transf.* **1979**, *22*, 547–556.
22. Pradesh, A. Process Design Rotary Dryer. Available online: http://www.sbioinformatics.com/design_thesis/Terephthalic_acid/Terephthalic-2520acid_Design-2520of-2520Equipments.pdf (accessed on 20 September 2014).
23. Duman, G.; Azhar Uddin, M.; Yanik, J. Hydrogen production from algal biomass via steam gasification. *Bioresour. Technol.* **2014**, *166*, 24–30.
24. Parparita, E.; Ashar Uddin, M.; Watanabe, T.; Kato, Y.; Yanik, J.; Vasile, C. Gas production by steam gasification of polypropylene/biomass waste composites in a dual-bed reactor. *J. Mater. Cycles Waste Manag.* **2014**, doi:10.1007/s10163-014-0308-0.

25. Gu, Z.; Li, K.; Qing, S.; Zhu, X.; Wei, Y.; Li, Y.; Wang, H. Enhanced reducibility and redox stability of Fe_2O_3 in the presence of CeO_2 nanoparticles. *RSC Adv.* **2014**, *4*, 47191–47199.
26. Kunii, D.; Levenspiel, O. *Fluidization Engineering*, 2nd ed.; Butterworth-Heinemann: Waltham, MA, USA, 1991.
27. Craig, K.R.; Mann, M.K. *Cost and Performance Analysis of Biomass-Based Integrated Gasification Combined Cycle (BIGCC) Power Systems*; NREL/TP-430-21657; National Renewable Energy Laboratory: Golden, CO, USA, 1996.
28. Sato, N. *Chemical Energy and Exergy*; Elsevier: Amsterdam, The Netherlands, 2004.
29. Gao, K.; McKinley, K.R. Use of macroalgae for marine biomass production and CO_2 remediation: A review. *J. Appl. Phycol.* **1994**, *6*, 45–60.
30. Brinkhuis, B.H.; Levine, H.G.; Schlenk, G.G.; Tobin, S. *Laminaria* cultivation in the far east and North America. In *Seaweed Cultivation for Renewable Resources*; Bird, K.T., Benson, P.H., Eds.; Elsevier: Amsterdam, The Netherlands, 1987; pp. 107–146.